Binding the Tobacco Mosaic Virus to Inorganic Surfaces

M. Knez,[†] M. P. Sumser,[‡] A. M. Bittner,*[,†] C. Wege,[‡] H. Jeske,[‡] D. M. P. Hoffmann,[†] K. Kuhnke,[†] and K. Kern[†]

Max-Planck-Institut für Festkörperforschung, Heisenbergstrasse 1, D-70569 Stuttgart, Germany, and Universität Stuttgart, Biologisches Institut, Pfaffenwaldring 57, D-70550 Stuttgart, Germany

Received August 5, 2003. In Final Form: November 6, 2003

We studied the adsorption behavior and surface chemistry of the tobacco mosaic virus (TMV) on well-defined metal and insulator surfaces. TMV serves as a tubular supramolecular model system with precisely known surface termination. We show that if the surface chemistry of the substrate and the pH-dependent chemistry of the molecular surface match, for example, by hydrogen bonding, a strong adsorption occurs, and lateral movement is impeded. Due to the immobilization, the virion can be imaged by atomic force microscopy (AFM) in contact mode. We also used self-assembled monolayers with an acyl chloride group to induce covalent bonding via ester formation. Noncontact AFM proved that TMV keeps its cylindrical cross section only under weak adsorption conditions, that is, on hydrophobic surfaces, while on hydrophilic substrates a deformation occurs to maximize the number of interacting chemical groups.

Introduction

The adsorption and bonding of biomolecules to all types of substrate surfaces is a central problem in fundamental studies, but also in biotechnological applications. Studies on typical "application surfaces" such as silicon wafers are ideally complemented by studies on highly defined single-crystal surfaces with atomic force microscopy (AFM). We aim to bind biomolecules to surfaces and to use them as templates for chemical reactions. For this, we have to focus on structures with exceptionally high chemical and physical stability such as the 300 nm long tubular *tobacco mosaic virus* (TMV).[1−4,44] Temperatures up to 90 °C[5] and pH values from 3.5 up to about 9 leave the structure largely unaffected for several hours,[6] and TMV is compatible with several polar solvents and can undergo organic reactions.[7,8] Such a combination of stability and versatility can only be reached by few other biomolecules, for example, by DNA (which is intensely investigated even under harsh conditions such as vacuum,[9] low temperatures,[10] or high forces[11]), by S layer proteins,[12] or by the bovine spongiform encephalopathy (BSE) protein.[13]

In contrast to older reports,[14,18,25−35] we present here a measurement of the AFM height of TMV on a range of chemically different surfaces. The circular rod shape (diameter, 18 nm) of the adsorbed virion was found only for graphite surfaces under investigation with noncontact AFM.[44] For pretreated glass and silicon surfaces and for gold and mica single-crystal surfaces, the shape appeared to be flattened (less than 15 nm height), which contradicts several older reports.[18,25−30] We also employed self-assembled monolayers (SAMs) on gold. Their carboxylate and acyl chloride termini can form covalent bonds with TMV. We carefully monitored the interaction of the AFM

* To whom correspondence should be addressed. Tel: (+49) 711/689-1433. Fax: (+49) 711/689-1079. E-mail: a.bittner@fkf.mpg.de.

[†] Max-Planck-Institut für Festkörperforschung.

[‡] Universität Stuttgart, Biologisches Institut.

(1) Knez, M.; Sumser, M.; Bittner, A. M.; Wege, C.; Jeske, H.; Kooi, S.; Burghard, M.; Kern, K. *J. Electroanal. Chem.* **2002**, *522*, 70.

(2) Henrick, K.; Thornton, J. M. *Trends Biochem. Sci.* **1998**, *23*, 358.

(3) Namba, K.; Pattanayek, R.; Stubbs, G. *J. Mol. Biol.* **1989**, *208*, 307.

(4) Pattanayek, R.; Stubbs, G. *J. Mol. Biol.* **1992**, *228*, 516.

(5) Zaitlin, M. *Tobacco Mosaic Virus, AAB Descriptions of Plant Viruses* **2000**, *370*, 8.

(6) Perham, R. N.; Wilson, T. M. A. *Virology* **1978**, *84*, 293.

(7) Wilson, T. M. A.; Perham, R. N. *Virology* **1985**, *140*, 21.

(8) King, L.; Leberman, R. *Biochim. Biophys. Acta* **1973**, *322*, 279.

(9) Fink, H.-W.; Schönenberger, C. *Nature* **1999**, *398*, 407.

(10) Porath, D.; Bezryadin, A.; de Vries, S.; Dekker, C. *Nature* **2000**, *403*, 635.

(11) Strick, T. R.; Allemand, J.-F.; Bensimon, D.; Bensimon, A.; Croquette, V. *Science* **1996**, *271*, 1835.

(12) Sleytr, U. B.; Bayley, H.; Sára, M.; Breitwieser, A.; Küpcü, S.; Mader, C.; Weigert, S.; Unger, F. M.; Messner, P.; Jahn-Schmid, B.; Schuster, B.; Pum, D.; Douglas, K.; Clark, N. A.; Moore, J. T.; Winningham, T. A.; Levy, S.; Frithsen, I.; Pankovc, J.; Beale, P.; Gillis, H. P.; Choutov, D. A.; Martin, K. P. *FEMS Microbiol. Rev.* **1997**, *20*, 151.

(13) Appel, T. R.; Wolff, M.; von Rheinbaben, F.; Heinzel, M.; Riesner, D. *J. Gen. Virol.* **2001**, *82*, 465.

(14) Drygin, Y. F.; Bordunova, O. A.; Gallyamov, M. O.; Yaminsky, I. V. *FEBS Lett.* **1998**, *425*, 217.

(15) Nicolaieff, A.; Lebeurier, G. *Mol. Gen. Genet.* **1979**, *171*, 327.

(16) Müller, D. J.; Engel, A.; Amrein, M. *Biosens. Bioelectron.* **1997**, *12*, 867.

(17) Anselmetti, D.; Dreier, M.; Lüthi, R.; Richmond, T.; Meyer, E.; Frommer, J.; Güntherodt, H.-J. *J. Vac. Sci. Technol., B* **1994**, *12*, 1500.

(18) Falvo, M. R.; Washburn, S.; Superfine, R.; Finch, M.; Brooks, F. P., Jr.; Chi, V.; Taylor, R. M., II *Biophys. J.* **1997**, *72*, 1396.

(19) Duevel, R. V.; Corn, R. M. *Anal. Chem.* **1992**, *64*, 337.

(20) Baker, M. V.; Landau, J. *Aust. J. Chem.* **1995**, *48*, 1201.

(21) Stubbs, G. *Philos. Trans. R. Soc. London, Ser. B* **1999**, *354*, 551.

(22) *Matthew's Plant Virology*, 4th ed.; Hull, R., Ed.; Academic Press: London, 2002.

(23) Klug, A. *Philos. Trans. R. Soc. London, Ser. B* **1999**, *354*, 531.

(24) Bhyravbhatla, B.; Watowich, S. J.; Caspar, D. L. D. *Biophys. J.* **1998**, *74*, 604.

(25) Anselmetti, D.; Lüthi, R.; Meyer, E.; Richmond, T.; Dreier, M.; Frommer, J. E.; Güntherodt, H.-J. *Nanotechnology* **1994**, *5*, 87.

(26) Schabert, F. A.; Rabe, J. P. *Biophys. J.* **1996**, *70*, 1514.

(27) Sit, P. S.; Marchant, R. E. *Thromb. Haemostasis* **1999**, *82*, 1053.

(28) Maeda, H. *Langmuir* **1997**, *13*, 4150.

(29) Imai, K.; Yoshimura, K.; Tomitori, M.; Nishikawa, O.; Kokawa, R.; Yamamoto, M.; Kobayashi, M.; Ikai, A. *Jpn. J. Appl. Phys.* **1993**, *32*, 2962.

(30) Thundat, T.; Zheng, X.-Y.; Sharp, S. L.; Allison, D. P.; Warmack, R. J.; Joy, D. C.; Ferrell, T. L. *Scanning Microsc.* **1992**, *6*, 903.

(31) Zenhausern, F.; Adrian, M.; Emch, R.; Taborelli, M.; Jobin, M.; Descouts, P. *Ultramicroscopy* **1992**, *42−44*, 1168.

(32) Zenhausern, F.; Adrian, M.; ten Heggeler-Bordier, B.; Ardizzoni, F.; Descouts, P. *J. Appl. Phys.* **1993**, *73*, 7232.

(33) Wadu-Mesthrige, K.; Pati, B.; McClain, W. M.; Liu, G.-Y. *Langmuir* **1996**, *12*, 3511.

(34) Vesenka, J.; Manne, S.; Giberson, R.; Marsh, T.; Henderson, E. *Biophys. J.* **1993**, *65*, 992.

(35) Bushell, G. R.; Watson, G. S.; Holt, S. A.; Myhra, S. *J. Microsc.* **1995**, *180*, 174.

10.1021/la035425o CCC: $27.50
Published on Web 12/10/2003

tip and the virion and found conditions that allowed stepwise mechanical destruction, "shaving", without complete dissection as in ref 18. We propose a classification of the predominant forces on different substrates, after distinct treatments, into weak (van der Waals type), hydrophilic (mainly based on hydrogen bonds), and covalent bonding.

Experimental Details

A suspension of TMV *vulgare* was employed to mechanically infect *Nicotiana tabacum* cv. Samsun nn by treating leaves with carborund. After 4 weeks, systemically infected leaves were harvested and stored at −20 °C. Two methods were employed to isolate the virion, including centrifugation in either CsCl or sucrose gradients, yielding 10 mg/mL TMV suspensions in water which were stored at 3 °C. In some cases, we replaced water by Na-K-phosphate buffer (pH 7) prepared from 10 mM Na_2HPO_4 + 10 mM KH_2PO_4. We found considerable degradation (particles < 300 nm long) after several months of storage.

Silicon wafers ((100) orientation, Crystal, Berlin) were terminated by SiO_2 with hydroxyl groups by the standard RCA procedure: 15 min of immersion into a 70−80 °C hot 1:1:5 mixture of 25% NH_4OH (VLSI Selectipur, Merck), 31% H_2O_2 (VLSI Selectipur, Merck), and water (Millipore, 18 MΩ cm); 15 min of immersion into a 70−80 °C hot 1:1:5 mixture of 37% HCl (Suprapur, Merck), 31% H_2O_2, and water. Mica (Provac, Liechtenstein) was cut into squares. Mica and graphite (highly oriented pyrolytic graphite (HOPG), ZYA quality, NTMDT, Moscow) were freshly cleaved by use of adhesive tape. Mg^{2+}−mica was prepared by immersion of freshly cleaved mica into 0.1 or 1 M $MgCl_2$ for 5 min. Gold surfaces were provided either by evaporation of gold (300 °C, 0.5 nm/s, 130 nm) on preheated (300 °C) mica at ca. 10^{-6} mbar or by a (111)-oriented single crystal (Mateck, Jülich). In most cases, we worked with 0.1 mg/mL TMV. Up to 1 mg/mL yielded good results. Adsorption times varied from 5 to 20 min. Whenever a droplet was used, the sample was covered against evaporation.

The following solutions/solvents were employed: $MgCl_2$ (Aldrich) in water (Millipore or Barnstead Nanopure, 18.2 MΩ cm), HCl (Merck 30% Suprapur), H_2SO_4 (Merck 95−97% Selectipur), $HClO_4$ (Merck 70% Suprapur), NaH_2PO_2 (Fluka p.a. ≥98%), 2-propanol (Merck VLSI Selectipur), dimethyl sulfoxide (DMSO, Merck Uvasol), toluene (Merck p.a.), ethanol (Roth Rotipuran ≥99.8% p.a.), 16-mercapto-hexadecanoic acid (Aldrich 90%), and $SOCl_2$ (Fluka puriss.).

Formation of a Reactive Acyl Chloride Terminated SAM. Flame-annealed Au/mica was immersed into an ethanolic solution of 16-mercapto-hexadecanoic acid ($HS-(CH_2)_{15}-COOH$). After ca. 12 h, the sample was removed, rinsed with ethanol and water, dried in an Ar stream, and placed in a glass apparatus. After evacuation (0.01 mbar), $SOCl_2$ vapor was purified by evaporation and condensation into a flask cooled to −196 °C. $SOCl_2$ was then warmed, and the vapor was passed over the sample (25 °C) before being condensed into a second cold flask. The sample was removed in a stream of Ar and immediately used.

For in situ AFM, we employed a Molecular Imaging Pico SPM with CSC12 AFM tips (NTMDT, silicon cantilevers). For AFM in air, we worked with a Thermomicroscopes M5 Autoprobe with Park Scientific Ultrasharp, MikroMasch NSC11 and CSC12, and Nanosensors NCHR and CONTR tips. Noncontact AFM at 60−300 kHz was done with drive frequencies above or below the resonance frequency; the latter case corresponds to intermittent contact behavior.

For transmission electron microscopy (TEM), we employed a Zeiss EM 10 at 60 kV and a Philips CM 200 at 200 kV. Copper and nickel grids were coated with pioloform films (Plano; Plannet, Wetzlar) by standard procedures. Carbon was evaporated onto the coated grids at 2×10^{-5} mbar. For TEM experiments, these grids were dipped into ethanol and air-dried prior to use.

Sample Application and Negative Staining with Uranyl Acetate. Twenty microliters of a 0.2−0.5 mg/mL TMV suspension was placed on a TEM grid for 30 s and then washed with water. Two percent $UO_2(CH_3COO)_2 \cdot 2H_2O$ (Merck) and 0.5 mg/mL bacitracin (Sigma) were mixed 1:1 and centrifuged for 5 min at 14 000*g*. Twenty microliters of this solution was placed on the grid for 30 s. Surplus liquid was removed with paper, and the grid was washed with a droplet of water.

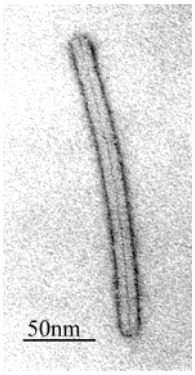

Figure 1. TEM (60 kV) image of a virion, negatively stained with uranyl acetate. The outer surface as well as the inner channel appear dark, i.e., uranyl-rich.

Infrared spectra of organic layers were aquired at 80° incidence with a Bruker IFS 66 spectrometer equipped with a nitrogen-cooled MCT detector. The reference was either flame-annealed gold or the same coated with a perdeuteriothiolate. Ellipsometry was performed with an EL X-02C ellipsometer (DRE, Ratzeburg). The ellipticity of the HeNe laser beam (633 nm) was minimized with a $\lambda/4$ plate, and the incidence angle was 70°. All uncoated gold samples had to be measured at more than four locations to calculate the complex index of refraction. After coating with an organic layer, the new data were fit to a model comprising this complex index of refraction and a layer with the purely real index $n = 1.45$ (nonabsorbing organic substance). In this way, the thickness of the layer was calculated.

The level of virion rod degradation by solvents was tested by contacting mica or Mg^{2+}−mica with the respective virion suspension, followed by noncontact AFM. An aqueous suspension of TMV could be treated with buffers and acids (pH 2.5 (at least for short times) up to 9) without destruction of the virion.[5] The solvents 2-propanol, tetrahydrofuran (THF), acetone, or DMSO could be added to the suspension or the dry virion could be suspended in them without structural change. However, THF at >30% in water and DMSO (which has to be added slowly due to the temperature rise!) at >70% in water both destroyed the virion. A partial stripping of the viral RNA, that is, polar disassembly of the virion capsid, is achieved with 70−80% DMSO.[14,15]

Results and Discussion

To classify bond strength into three categories from weak to covalent, a simple classification is provided by the amount of virions that adsorb to the substrate (valid when the virion approaches the substrate without an energetic barrier, i.e., without the electric double-layer repulsion).[16] This necessitates contacting the virion suspension with the substrate for a certain time and then removing the suspension, and in some cases additionally rinsing with virion-free solution. In the absence of kinetic effects, the higher the density on the substrate, the higher the bond strength. To elucidate kinetic effects, we varied the immersion time; in the following we will mention these experiments only when an effect (i.e., reduced adsorption at short immersion times, observed for graphite and for gold above pH 4) was observed.

Different TMV−substrate interaction strengths yield different noncontact or intermittent contact AFM heights. In contrast, the width can only be estimated roughly since it depends strongly on the tip shape. We thus made use of the fact that TEM is a complementary method. Generally, we found widths that were too large by AFM (e.g., 80 nm) but the correct 18 nm by TEM. The TEM image in Figure 1 shows a dark outer surface (outline) as

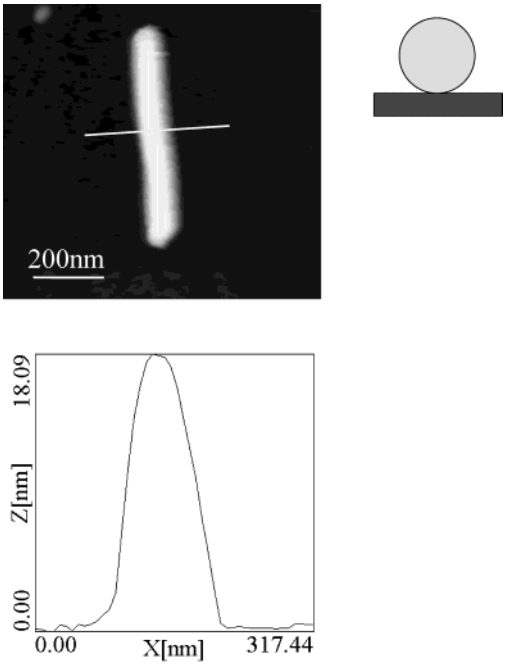

Figure 2. Noncontact AFM of two virions in linear arrangement on graphite. The measured height of 18 nm corresponds to the true diameter, while the width (ca. 85 nm (fwhm)) is attributed to the AFM tip shape. The true width can be detected with TEM (Figure 1). The adsorption was from a 40% DMSO aqueous suspension (0.1 mg/mL virions).

well as a dark inner channel (line), proving that the employed uranyl acetate stains the channel and is also deposited along the outer protein surface (negative contrast). The basis for the interpretation of our experiments is the chemical nature of the virion surface that interacts with the substrate surface.[2−5,21−23] The capsid proteins display only alkyl and hydroxyl groups and their C-termini (carboxylate groups) at the outer virion surface.[24] Some water molecules are so tightly bound that they can be resolved in diffraction studies of "dry" crystals.[2−4]

1. Weak Bonding. We first consider the "weak bonding" regime, which may in fact be true physisorption. A good criterion for weak bonding was if the virion could be imaged by noncontact AFM, but only with difficulties or not by intermittent contact AFM, while contact AFM with forces in the nanoNewton range always displaced TMV. Note that we never observed bending of the virion (which can be induced by inhomogeneous surfaces)[17] on any of the substrates tested.

HOPG with its hydrophobic and unreactive surface offers pure van der Waals bonding. Here kinetics plays a role: The adsorption is rather slow, and high coverages can only be realized by leaving a droplet to dry on graphite.[18] The sluggish kinetics may be explained based on colloid effects: A repulsive interaction (barrier) between a surface and a colloid or virus is postulated since at least the latter is surrounded by an electric double layer.[16] We found that TMV adsorbed faster from a suspension in 40% DMSO in water. Only noncontact AFM worked well: Figure 2 displays two head-to-tail aggregated virions (600 nm in length) as a bright line, that is, as a protrusion, on the substrate.[44] The horizontal scan line across the diameter shows a width (here ca. 85 nm) that strongly depends on tip quality and thus is difficult to interpret. The measured height was 18 nm. In cases of higher coverage of the surface with TMV, the virions start to aggregate randomly, leading to a higher stability of the thus-formed "virion grid" on graphite. Only then was intermittent contact mode AFM imaging possible.

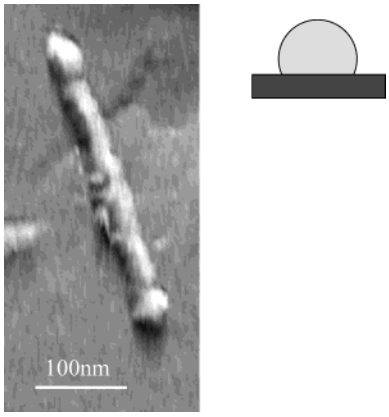

Figure 3. In situ contact AFM. An error mode image of TMV adsorbed on Au(111) in aqueous acetic acid (pH 4) is shown. The maximum height of the particle is 10 nm, but height differences within one single particle can reach 4 nm.

The fact that contact AFM moves/slides the virion but non- or intermittent contact AFM does not would appear logical for small molecules, but even the weakest interactions (van der Waals) amount to considerable bond energies for large molecules, for example, 8 kJ/mol per nm length of a 10 nm diameter carbon tube.[39] In addition, such interactions are not directional and should prevent vertical detachment with a tip as well as sliding. However, Si or Si_3N_4 AFM tips have more or less hydrophilic hydroxyl layers that cause large dipole−dipole forces between the tip and the virion surface. Only when the tip is very sharp and the surface very flat should the van der Waals forces between the virion and the substrate be larger.

2. Hydrophilic Bonding. Imaging of TMV in contact mode AFM was achieved after treatment of the virion suspension with HCl, H_2SO_4, $HClO_4$, and CH_3COOH of pH 4 and adsorption on hydroxyl-containing surfaces such as oxidized silicon wafers, mica, or glass (gold in laboratory air is covered by a very thin water layer and is thus also hydrophilic). In none of these experiments did we find a significant difference in the virion behavior. Figure 3 is an in situ error mode AFM image (the appearance resembles the derivative of the horizontal scan lines); hence the virion appears as a black (the tip moves toward the surface) and white (the tip moves away from the surface) line. The apparent virion width varies over its length. Some structures of the underlying gold crystal can be seen, for example, a multiatomic step that runs roughly normal to the virion axis at its upper third. Figure 4 is an AFM image of TMV on gold after adsorption from a suspension with extremely low pH (2.8). The virion, appearing as a bright line, has preserved its structure (but not its height). In general, images recorded in contact mode AFM on gold (Figures 3 and 4) had poor resolution so that noncontact mode imaging is preferable; as the experiments on HOPG show, noncontact AFM is required for a correct height determination. However, the facts that contact mode AFM imaging is possible (although only at

(36) Guckenberger, R.; Arce, F. T.; Hillebrand, A.; Hartmann, T. *J. Vac. Sci. Technol., B* **1994**, *12*, 1508.
(37) Mantovani, J. G.; Allison, D. P.; Warmack, R. J.; Ferrell, T. L.; Ford, J. R.; Manos, R. E.; Thompson, J. R.; Reddick, B. B.; Jacobson, K. B. *J. Microsc.* **1990**, *158*, 109.
(38) Nony, L.; Cohen-Bouhacina, T.; Aimé, J.-P. *Surf. Sci.* **2002**, *499*, 152.
(39) Hertel, T.; Walkup, R. E.; Avouris, P. *Phys. Rev. B* **1998**, *58*, 13870.

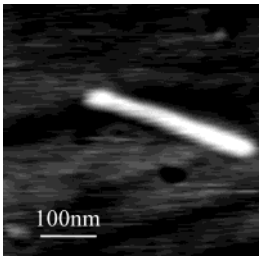

Figure 4. Contact AFM of TMV adsorbed on Au(111) from aqueous HCl (pH 2.8). Note that the virion is intact despite the very acidic conditions during adsorption.

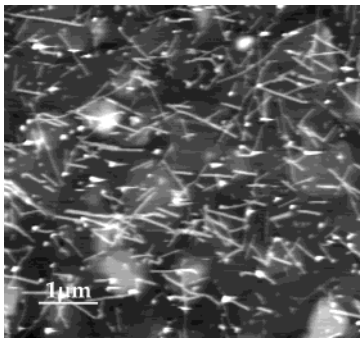

Figure 5. Contact AFM of TMV adsorbed on freshly cleaved mica from aqueous HCl (pH 2.8). Note that many virion rods are intact despite the very acidic conditions during adsorption. The height differences between the virions and within a single virion do not exceed 3 nm.

low forces) and that it improves with decreasing pH show that the bonding of the virion to the surface is much stronger than on HOPG.

Figure 5 shows a contact AFM image of a mica surface after adsorption of virions from a suspension with extremely low pH (2.8); the virions are clearly discernible as bright lines. In many cases, the lines are longer than 300 nm, pointing toward head-to-tail (linear) aggregation.[44] The white (very high) horizontal streaks may be attributed to protein material picked up by the scanning tip. These streaks are frequently observed with contact AFM, while we rarely observed them in noncontact mode. We can conclude that at pH values lower than about 4 imaging up to several nanoNewtons becomes possible on gold (Figures 3 and 4) but also on mica (Figure 5). For the case of Au(111), we tested HCl, H_2SO_4, $HClO_4$, and CH_3COOH and found no difference; that is, non- or intermittent contact AFM resembled the results mentioned above, and contact AFM could yield images (Figure 4). The apparent height was below 12 nm. Kinetic effects became obvious at pH values above 4; indeed, adsorption was barely noticeable even after long incubation times (compare to HOPG in section 1).

Silicon wafers (cleaned oxidatively with the standard RCA procedure), glass, and a 16-mercapto-hexadecanoic acid ($HS-(CH_2)_{15}-COOH$) SAM on Au showed very similar results (images not shown). However, coverages were difficult to reproduce, and the optimum pH values depended slightly on the substrate type. Mg^{2+}-treated mica (mica covered by strongly adsorbed Mg^{2+} ions, see the experimental section) was an especially effective substrate for hydrophilic bonding (see Figure 6). The measured height (15 nm) was again clearly below the ideal 18 nm.

The interpretation of these results is based on the pH-dependent surface chemistry of TMV: Above pH 3.5, the overall charge of TMV is negative, but the carboxylate groups on the outer surface are protonated, and hydrogen bonds to hydroxyl surfaces such as mica readily form. To

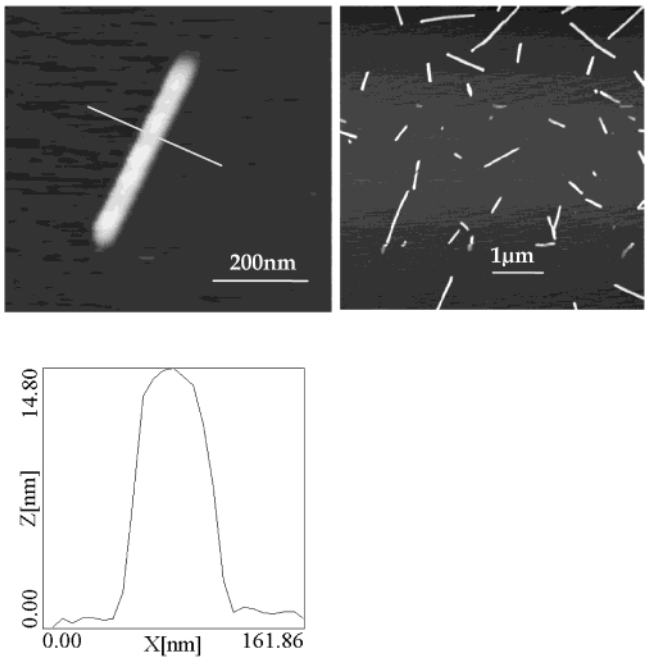

Figure 6. TMV on Mg^{2+}-treated mica, in intermittant contact mode. Note the relatively low apparent height and the head-to-tail arrangement leading to extended linear structures. The height differences between the virions and within a single virion do not exceed 2 nm.

maximize the number of bonds, TMV deforms and thus a smaller height is found. Contact AFM is possible since the forces between the tip and TMV are smaller than between TMV and the substrate, simply due to the small contact area of the tip. Above pH 5, the outer surface becomes deprotonated and thus negatively charged. The charge and counterions from the electrolyte should result in a thinner double layer and less repulsion. Again, hydrogen bonds to surface hydroxyl groups could develop. In contrast to silicon wafers and mica, on gold only small coverage is attainable, even after prolonged exposure. While protonated TMV should adsorb on gold in analogy to uncharged molecules (carboxylic acids readily adsorb on gold[41]), highly charged objects such as deprotonated TMV cannot adsorb, even when they overcome the above-mentioned kinetic barrier. Anions can adsorb strongly only when they are partially or fully discharged on metal surfaces: For example, S^{2-} or I^- adsorb strongly and are discharged[45] while ClO_4^- adsorbs weakly and retains its charge.

TMV shows aggregation in the presence of bivalent cations such as Cd^{2+}, Zn^{2+}, Pb^{2+}, Cu^{2+}, and Ni^{2+}.[40] The presence of Mg^{2+} on the substrate (attached by complex formation with the hydroxyl termini of the mica) leads to a similar effect: The remaining half shell of water ligands at Mg^{2+} can be substituted by hydroxyl and carboxylate groups of the virion surface; in other words, a salt bridge between mica and virion forms. Indeed, we find that TMV at mica surfaces is tightly bound and can be scanned at high forces.[18]

(40) Nedoluzhko, A.; Douglas, T. *J. Inorg. Biochem.* **2001**, *84*, 233.
(41) Han, S. W.; Joo, S. W.; Ha, T. H.; Kim, Y.; Kim, K. *J. Phys. Chem. B* **2000**, *104*, 11987.
(42) Epple, M.; Bittner, A. M.; Kuhnke, K.; Kern, K. *Langmuir* **2002**, *18*, 773.
(43) Bittner, A. M.; Epple, M.; Kuhnke, K.; Houriet, R.; Heusler, A.; Vogel, H.; Seitsonen, A. P.; Kern, K. *J. Electroanal. Chem.* **2003**, *550−551*, 113.
(44) Knez, M.; Bittner, A. M.; Boes, F.; Wege, C.; Jeske, H.; Mai*β*, E.; Kern, K. *Nano Lett.* **2003**, *3*, 1079.
(45) Magnussen, O. M. *Chem. Rev.* **2002**, *102*, 679.

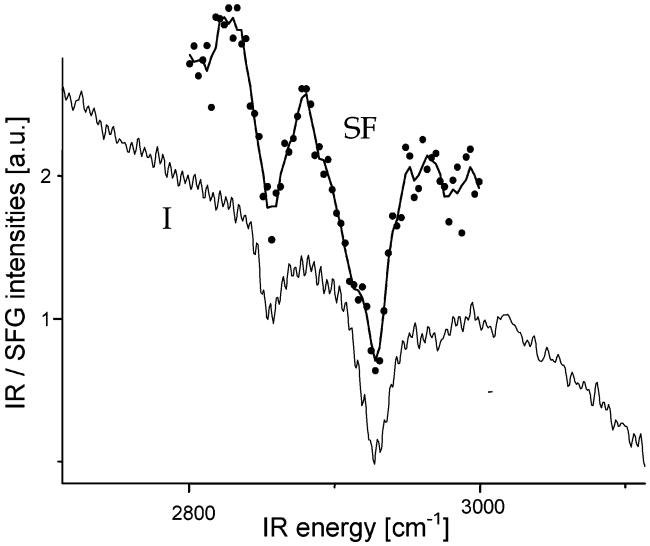

Figure 7. Infrared (IR, line) and infrared−visible sum frequency spectra (SFG, dots) of $HOOC(CH_2)_{15}S/Au(111)$. Symmetric and asymmetric methylene stretch bands are well detectable, very broad, and shifted to higher energy as compared to those of alkanethiolates.

3. Covalent Bonding. We first characterized an $HS-(CH_2)_{15}-COOH$ SAM on Au (see the experimental section) by infrared spectroscopy, by spectroscopic infrared−visible sum frequency generation, and by ellipsometry. In detail, we detected the two methylene stretching vibrations at 2855 cm^{-1} (full width at half-maximum (fwhm) of 15−20 cm^{-1}) and 2925 cm^{-1} (25−30 cm^{-1}) (Figure 7) in infrared and also in sum frequency spectra. The sum frequency peaks are ca. 10 cm^{-1} wider. In the investigated range (ca. 2000 to ca. 3200 cm^{-1}), no other vibrations were detected. Ellipsometry yielded a nominal thickness of 1.8−2.1 nm. It is important to understand that a SAM can easily change its conformation when it comes into contact with molecules. In fact, even a slow and nondestructive deposition of copper atoms can alter the conformation completely.[42] In our case, however, the SAM is already distorted: The positive shift of the C−H vibrations (as compared to all-trans methylene chains) points toward substantial disorder. Nevertheless, the ellipsometric thickness is well comparable with that of alkanethiolates of similar length; hence the SAM is dense. Our interpretation is that intermolecular hydrogen bonds (and most likely also adsorption of water) are energetically so much favored that defects build up in the C_{15} chains in order to allow for as many hydrogen bonds as possible (Figure 8). The chains are thus bent (presumably even more than one C−C bond per chain is twisted), and they also point in different directions. This is verified by the sum frequency spectra: Their appearance resembles the infrared spectra very much. This first appears surprising because methylene resonances are symmetry-forbidden and thus not observed when the chain is in the all-trans conformation (as for alkanethiolates on gold).[42] Indeed, the occurrence of the methylene peaks is direct proof for disorder. The peak intensities are larger than those of methyl peaks from alkylthiolates, so we can infer multiple gauche defects in the methylene chain, as we also showed for an amino-amido-thiolate monolayer.[43]

From this SAM, we synthesized a reactive SAM with an acyl chloride terminus (see the experimental section and refs 19 and 20). When contacted with a virus suspension, the fast reaction of water, whether in the bulk or at the virion surface, with this SAM competes with the ester formation between the acyl chloride and hydroxyl or carboxylate groups at the virion surface (Figure 8). But the number of ester bonds is sufficient to immobilize TMV: We were able to apply high forces in AFM without moving the adsorbed virion. We also checked for low-pH esterification of the $HS-(CH_2)_{15}-COOH$ SAM. After reaction with the virion suspension for at least 6 h at low pH, contact mode AFM measurements showed approximately half the amount of virion (compared to the acyl chloride method) tightly bound to the surface. We assume that the bonding of the virion with the SAM is again via an ester.

A chemically resilient virion such as TMV can be expected to show also unusual mechanical stability. For the covalently bound virion, contact AFM in air was possible even at high setpoint forces. A typical result is shown in Figure 9 where we employed lateral force mode detection to enhance the contrast (this results in a derivative-like appearance of the scan lines, that is, the virion resembles a black−white rod). At low forces (nominally <10 nN), the images show TMV with a height of about 13 nm and a length of 410 nm. The difference in length compared to the length obtained by TEM results

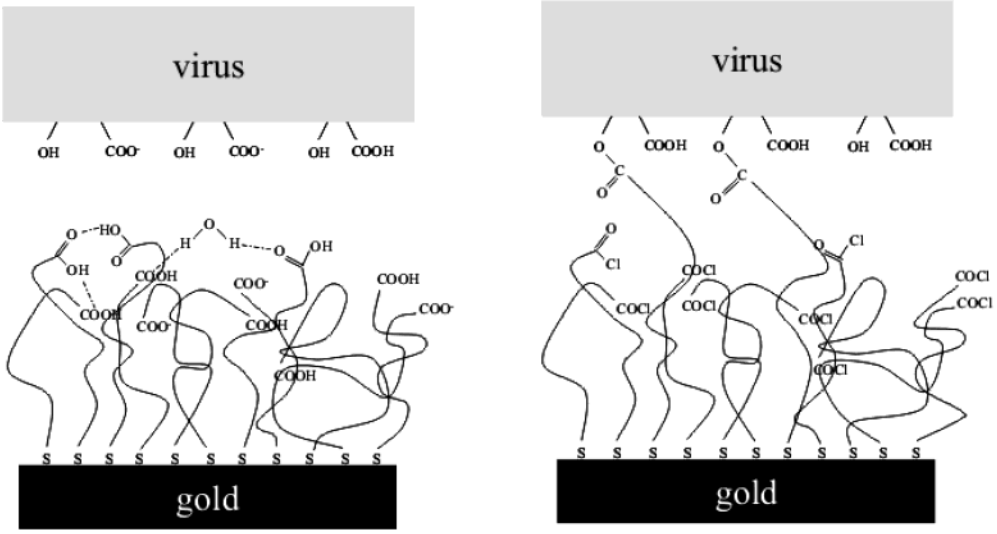

Figure 8. Left: Model of the $HOOC(CH_2)_{15}S/Au(111)$ layer, based on ellipsometric and spectroscopic results (see Figure 7). The alkyl backbones are distorted by interchain hydrogen bonds. The virion is bound via hydrogen bonds. Right: Model of $ClOC(CH_2)_{15}S/Au(111)$. The acyl chloride groups can form covalent ester links with viral hydroxyl groups.

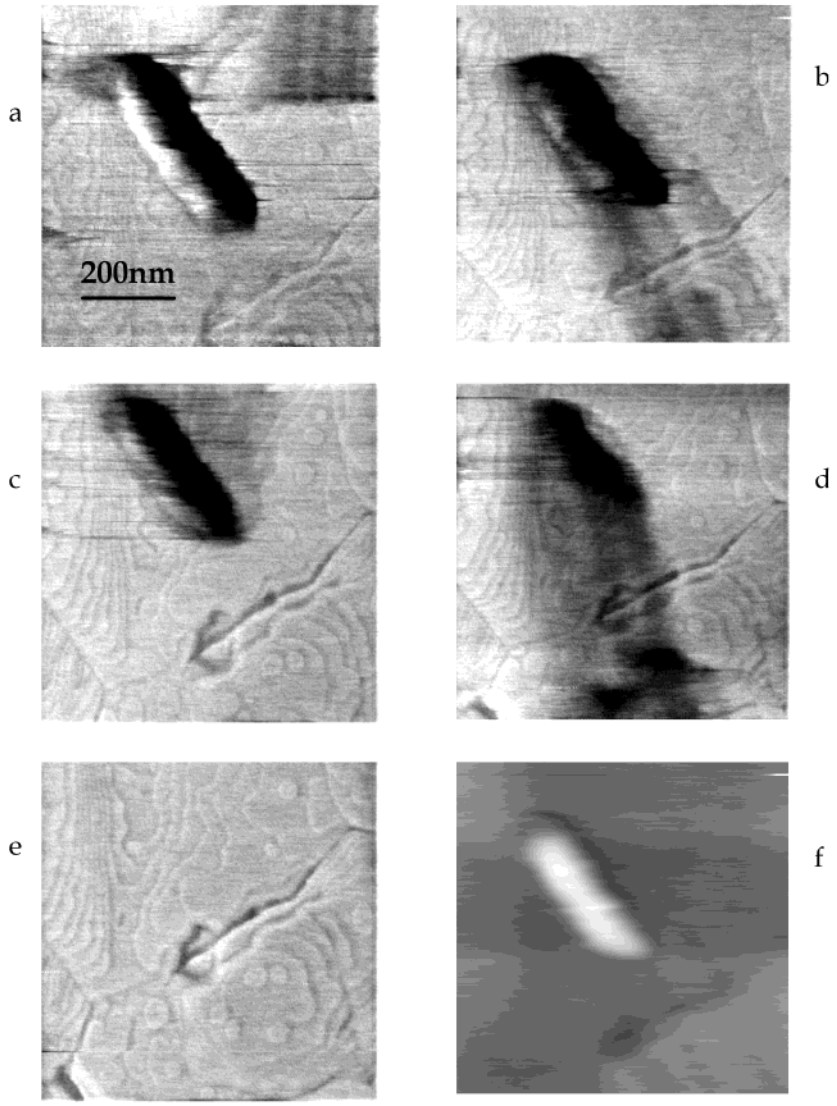

Figure 9. Sequence of contact AFM images in lateral force mode of covalently bound TMV on $ClOC(CH_2)_{15}S$/Au(111) ("sticky monolayer") under increasing load, recorded with a ca. 1 N/m force constant. Images a−e: 10, 30, 50, 80, and 100 nN. The last image was reproduced also at 10 nN. Step edges of the Au single crystal are visible as black lines especially in the lower right part. All images show a linear defect extending from the middle to the middle right part. Image f shows the same scan as image b, but in topography mode.

from the large tip curvature (convolution). The measured width at fwhm of the virion is 80−90 nm, which indicates a tip radius of ca. 35 nm. An increase above ca. 30 nN led to a small decrease of these values (shaving) and to the appearance of some features (lines) close to the virion with heights below ca. 0.5 nm. Finally, above ca. 50 nN we could only find some features of very low height at the location of the virion. Note that the gold steps (black lines especially in the lower right part) and a linear defect, extending from the middle to the middle right part, serve as markers. In some experiments, a contrast inversion (negative heights, the virion appears black) was found at intermediate setpoints (see Figure 9d). However, in each experiment the final result was similar, and returning to low forces did not change the image any further. Several elongated protrusions (e.g., the dark features covering the middle part of Figure 9d) pointed toward degraded virion material (e.g., Figure 9b, where next to the bottom part of the virion a black feature extends to the bottom right part of the image; the topographic mode shows a protrusion here). Furthermore, these protrusions appear to follow the slow (here downward) scan direction, which suggests that protein material from the tip was slowly deposited on the surface adjacent to the virion. The reverse was observed in upward scans (Figure 9c), that is, protrusions at the top of the image. The partially destroyed TMV, interacting with the tip, may have acted like a cleaning brush since no protrusions were observed in any image before the tip had encountered the virion at high force.

Imaging TMV with AFM. The non- and intermittent contact AFM heights we found for TMV depended slightly on the respective conditions, but all are at least 1 nm, often 4 nm smaller than the expected value of 18 nm (except for noncontact AFM on graphite) which is the TMV diameter as determined with TEM. The deformation of adsorbed TMV maximizes the number of bonds to the surface; similar observations were made with carbon nanotubes adsorbed on H-terminated Si(100).[39] Our measurements are in contrast to the data of refs 18 and 25−30, where the expected value (±1 nm) was found with AFM. On the other hand, many values from 9 to 23 nm are reported in other studies[14,31−35] or with scanning tunneling microscopy (STM).[36,37] Even under very similar conditions, reported heights vary up to 100%. We made sure that the height calibration of our AFM machines

was correct by scanning height standards such as Au(111) (see also Figure 9, monatomic steps of 0.24 nm), HF-etched mica (mica immersed in 40% HF for 1 h and then rinsed with water, 1.0 nm high steps), and a grating of known height (180 nm). We found that height values in the non- and intermittent contact modes can be several tens of percent too low when the feedback and drive settings are incorrect or when the tip is imperfect.

Water molecules in or at TMV alter its conductivity, as verified by STM, which is only successful above ca. 40% humidity.[36] Hence some of the discrepancies reported in the literature could be due to hydrated or dehydrated samples. Capillary forces, which are present at high humidity even for noncontact AFM,[38] can, in principle, differ on the bare substrate and on the virus, but usually both substrate and virus should be covered by one or several layers of water. A possibility to avoid capillary forces is to measure in situ, as we demonstrate in Figure 3.

We note that the compressibility of TMV plays a large role for contact AFM, and indeed low heights are encountered at high force setpoints. In this regime, the AFM tip can deform or penetrate the virion during scanning (in addition to its adsorption-related deformation); hence the height information is lost.

The isoelectric point of TMV is at pH 3.5.[5] Most of the AFM[18,25−29,31−35] and STM[36,37] work was done with neutral suspensions and hence with highly negatively charged virions. Since the exact distribution of charge depends on the protein sequence, the use of virions with slightly differing sequences, which is known for the naturally occurring strains, may well account for different heights. We exclude another source of errors, electrostatic tip charging, by employing highly doped tip material and by grounding the tips.

Conclusions

AFM experiments show that it is possible to image the TMV at solid−air and solid−liquid interfaces on well-defined substrates such as mica and Au(111). We clarified that the observed imaging heights from 10 to 18 nm depend on the substrate and the pH, while transmission electron microscopy always revealed a diameter of 18 nm. The AFM heights are due to a radial compressibility in connection with a "flattened" shape that results from the attachment of as many protein moieties as possible to the surface. The ideal height of 18 nm can be found on a substrate that offers only van der Waals type bonding (graphite) when scanned at minimum tip−sample interaction (noncontact AFM).

TMV can adsorb at metal (gold) as well as hydroxyl-containing surfaces (mica, glass, silicon wafer). We obtained adsorption of single virions by selecting conditions according to the substrate chemistry. The bond strength is large whenever hydrogen bonds can form, especially at pH values around 3 which are incompatible with many other biomolecules. An attachment employing Mg^{2+} and a covalent attachment to an acyl chloride terminated monolayer provide strong bonding although sum frequency generation spectroscopy shows conformational disorder of the chain. In the case of covalent attachment, AFM can effect a stepwise degradation of TMV by shaving off material.

Acknowledgment. We thank J. Kahl and Prof. Dr. H. U. Habermeier for the preparation of evaporated gold samples, W. König and Dr. J. Kuhl (all Max-Planck-Institut für Festkörperforschung) for acquiring infrared spectra, and C. Kocher for technical assistance; we thank F. Boes for his contribution to several solvent experiments; we gratefully acknowledge discussions with Prof. Dr. K. W. Mundry (all Universität Stuttgart).

LA035425O